

In situ measurement of batch glass during melting

Friedrich Raether and Manfred Krauß

Fraunhofer-Institut für Silicatiforschung (ISC), Würzburg (Germany)

A novel optical measuring method is described which was used for the density measurement of model samples of glass batch during the melting process. It used a sample volume of some 1000 mm³, which was sufficiently large to suppress single particle effects. Shape changes of batch samples during heating were taken into account by the optical method. Volumetric changes of soda-lime-silica glass batch were monitored between room temperature and 1100 °C. Initially a sintering stage was observed showing self similar reduction in the sample volume. Thereafter, the sample shape approached the equilibrium surface of drops. This was accompanied by a large increase in volume, which was attributed to the formation of gas bubbles within the batch samples. A strong influence of heating rate and composition on this volume increase was observed.

1. Introduction

Today the temperature and flow in large glass melting furnaces can be simulated on the computer using finite element methods. The numerical challenges in solving large models have been overcome by the dramatic increase in computer power [1 to 5]. The accuracy of the models is limited mainly due to the lack of precise high temperature material data which are required as input parameters. This particularly applies to the batch melting process. During the rapid heating of the batch in the melting furnace, thermal, chemical and viscous phenomena are closely interrelated. Starting from ambient temperature with a free-flowing powder mixture, material properties change dramatically, ending with a viscous liquid with trapped gases at the temperature of the glass melt. An overall modelling of batch melting by finite element methods has to simplify these complex processes. Because of that it is even more important to base the simulations on precise measuring data.

Usually the raw materials are fed onto the top of the melt where they form a thick layer of roughly 10 cm. Heating occurs from both sides by the glass melt underneath and the vault of the furnace above. Heating rates are between 10 and 50 K/min dependent on the position in the batch layer [6]. The interplay between the complex mechanisms during this rapid heating process essentially affects the homogeneity and quality of the glass melt. So the predominant part of gas release takes place during batch heating when gaseous species like CO₂ originating from decomposition of the raw materials can easily escape via open pore channels within the batch layer. Residual gases in the glass melt have

to be removed by additional fining. The formation of silica rich agglomerates during batch heating can produce knots of low solubility which have to be removed from the melt by prolonged heating cycles [7].

Already Tammann described batch melting as a sintering process [8]. Boccaccini investigated the sintering process of glass matrix composites containing particulate inclusion phases [9]. Since the driving force during sintering is the decrease in surface energy by the reduction in pores, the most important material property which governs sintering is density. The increase in density causes the well known sintering shrinkage. With ceramics and powder metals sintering shrinkage is usually measured by push rod dilatometry [10]. Yet, due to their small strength, push rod dilatometry cannot be applied to batch samples. Therefore, optical methods have been used [11]. In those early experiments the sample diameter was measured during heating of small batch samples in a hot stage light microscope. Additionally the microstructure was observed and the understanding of processes during the formation of the silicate melt was improved. But the accuracy of the shrinkage data was purely due to the small measuring volume which was used in the microscope images [11]. Different from those laboratory experiments in the melting furnace the hot glass melt can penetrate into the batch blanket driven by capillary forces. But the viscosity of the melt is so high that this process only affects the interface region between melt and batch layer [12 and 13]. This gives justification for model experiments where batch heating is investigated, using a batch heap without contact to the melt.

2. Experimental procedure

A horizontal tube furnace was used for the heating of the glass batch samples. The upper and the lower half shell were

Received 26 January 2004.

Presented in German at: 77th Annual Meeting of the German Society of Glass Technology (DGG) on 27 May 2003 in Leipzig (Germany).

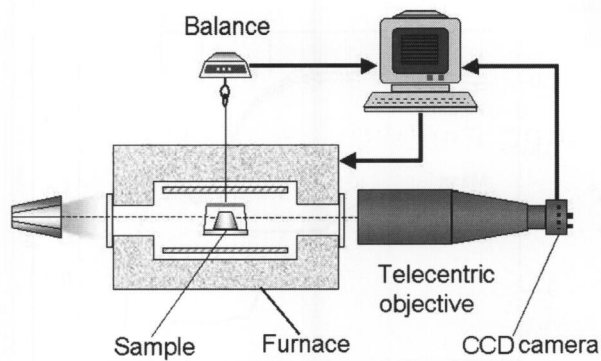


Figure 1. Setup of the in situ measuring furnace.

Table 1. Composition of the glass batches

| glass component | type 1 mass fraction in % | type 2 mass fraction in % | raw material |
|-------------------|---------------------------|---------------------------|--------------------|
| SiO ₂ | 74 | 37 | quartz |
| Na ₂ O | 16 | 8 | NaHCO ₃ |
| CaO | 10 | 5 | CaCO ₃ |
| glass frit | - | 50 | - |

heated separately. The inner diameter of the furnace was 285 mm and its length 340 mm. Maximal temperature was 1550 °C. Windows of quartz glass with a diameter of 50 mm were at the faces of the furnace (figure 1). The batch sample was positioned in the centre of the furnace. It was illuminated from one side by a halogen lamp. The silhouette of the sample was measured on the opposing side by a CCD camera. A telecentric optic avoided measuring errors due to a slight shift of the sample position which occurred frequently during heating of the furnace. Images of the CCD camera were stored every ten seconds on a personal computer. By averaging those images, optical distortions caused by temperature gradients and turbulence in the furnace atmosphere were eliminated. The lateral resolution achieved was 2 µm. The measuring method is described in detail in [14 and 15]. The sample holder was made of alumina. It was hung from a balance which was placed above the furnace (figure 1). The accuracy of the balance was ± 0.01 g (type: Sartorius CP 3202S, Sartorius AG, Göttingen (Germany)). The mass change during heating was recorded simultaneously to the shrinkage measurement.

Two different batch compositions were investigated (table 1). Customary raw materials for glass melting were used. The composition of type 1 batch was chosen to form a standard soda-lime-silica glass [16]. Such a glass was produced from type 1 batch by heating and homogenizing at 1500 °C and casting the melt on a metal plate to produce a glass frit. The glass frit was ground in a disc vibration mill and mixed in a 50 to 50 ratio with type 1 batch. This mixture was denoted type 2 batch. It was used as a model system for glass batches with a high fraction of cullet. The powders were carefully mixed in a plastic bottle and slightly moistened with water thereafter. Conically shaped samples

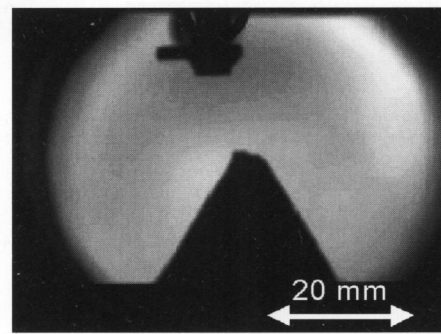


Figure 2. Image of a batch sample by the CCD camera of the optical dilatometer.

were formed from the powders by a plastic mould using only small manual pressure. The base diameter of the body was 28 mm and its height 20 mm. The initial weight of the samples was approximately 7 g. The initial pore volume determined from their density and the density of the raw materials was roughly 40 %.

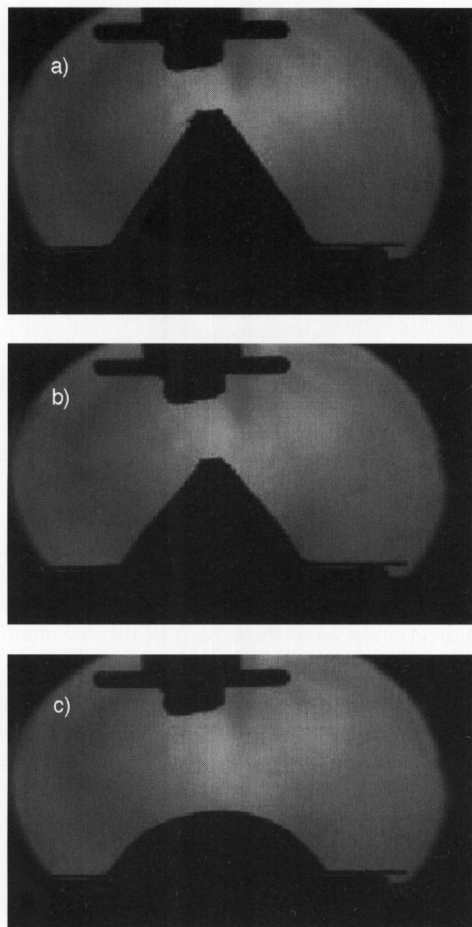
The samples were heated in air with a flow of 1 l/min at heating rates between 2 and 10 K/min. The measurements were stopped when the molten glass spread over the edges of the sample holder. (A crucible below the sample holder protected the furnace against the melt.) Some heating cycles were interrupted in advance at a temperature of 900 °C. In that case the hot samples were removed from the furnace and cooled rapidly in air to ambient temperature. Those samples were cut by a low speed saw and the inner surface was polished and examined in a scanning electron microscope (Type LEO 1450 VP LEO Elektronen-Mikroskopie GmbH, Oberkochen (Germany)) with a backscattered electron detector.

3. Data evaluation

Figure 2 shows an image of the batch sample. (The suspension of the sample holder is visible in the upper part of the image.) The silhouette of the sample was detected by a special contour tracking algorithm. The contour of the sample holder below the batch sample was lineally interpolated and subtracted. Since the samples were rotationally symmetrical, their volume could be calculated by rotating either the left or the right side of the contour around a vertical axis. (For geometric reasons using an axis through the centre of gravity of the sample area both sides yield the same volume.) The influence of a slight asymmetry of the sample contour was estimated by dividing the sample area in thin horizontal strips and choosing either only the smaller radii of the left and right side for the summation of the rotational volume or the larger radii, respectively. By that lower and upper bounds for the sample volume were determined. Relative volumes were used by dividing the calculated values by the respective values at the beginning of the heating process.

Density ρ was calculated from the measured sample weight M and relative volume V_{rel} by considering the volume V_{mould} of the frustum mould:

$$\rho = M / (V_{\text{rel}} \cdot V_{\text{mould}}). \quad (1)$$



Figures 3a to c. Images during heating of type 1 batch with a heating rate of 2 K/min at a) 815 °C, b) 935 °C, and c) 1005 °C.

Sample mass was divided by the respective mass measured at 500 °C since adsorbed water and hydrocarbonate decomposition resulted in deviations at low temperatures.

4. Results and discussion

Figures 3a to c show images of the batch sample (type 1) in different states of the heating process. The volumetric and mass changes during heating of that sample are shown in figure 4.

The decrease in mass begins at 700 °C and is essentially finished at 900 °C. It reflects the well known decomposition reactions of the carbonates used as raw materials and the formation of silicates. Thereby CO₂ is released to the furnace atmosphere [17 to 20]. The lower and upper bounds of the volume measurement ran closely within a range of initially 3%. The bounds became closer at higher temperatures when the surface roughness decreased.

Above 760 °C the sample volume decreased. A local volume minimum was passed at 935 °C and thereafter the volume increased until 1005 °C. At higher temperatures there was a rapid decrease in volume until the measurement had to be interrupted at 1120 °C because part of the glass melt spread out of the measuring window. Between 760 and

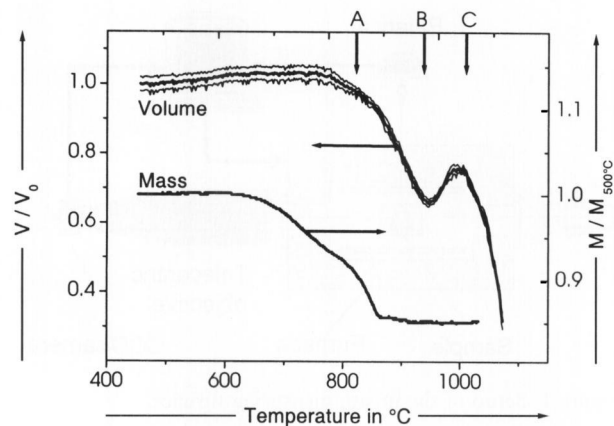


Figure 4. Volumetric change (V/V_0) and mass change ($M/M_{500\text{ }^\circ\text{C}}$) during heating of type 1 batch with 2 K/min. Upper and lower volume bounds are shown by thin lines. The temperatures of the images in figures 3a to c are indicated by arrows.

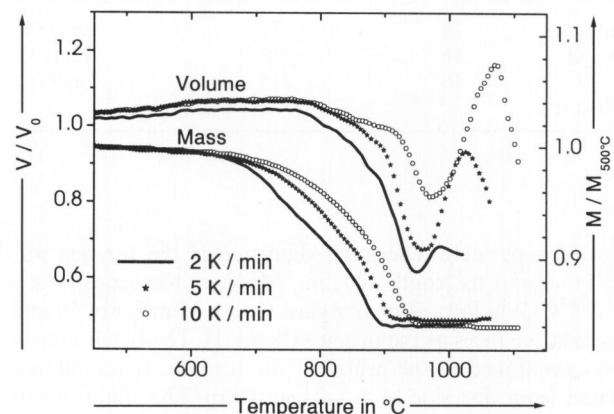


Figure 5. Volumetric and mass change during heating of type 1 batch with different heating rates.

935 °C the shape of the sample did not change whereas there was a large change towards a droplet silhouette between 935 and 1005 °C. (The temperatures which belong to the images in figures 3a to c are indicated in figure 4.) The self similar shrinkage below 935 °C corresponded to a usual sintering process. In this temperature range the solid fraction of the raw materials was sufficiently large to form a solid skeleton. At higher temperatures the liquid fraction increased and the viscosity of the batch sample became small enough to allow for the formation of an equilibrium surface shape. The increase in volume above 935 °C was attributed to the inclusion of bubbles. Although, above 900 °C the decrease in mass was below the detection limit, apparently bubble formation was strong enough to outweigh volume decrease by sintering.

Figure 5 shows the volume and mass change of samples heated at different heating rates. Increasing the heating rate from 2 to 10 K/min caused a shift of the mass and volume curves to approximately 80 K larger temperatures. The temperature gradient within the samples was estimated using a

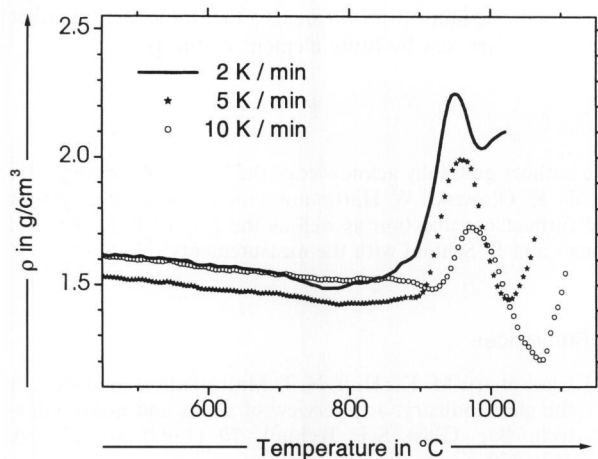


Figure 6. Density ρ during heating of type 1 batch with different heating rates.

thermal diffusivity of 0.1 and 0.4 mm²/s [6] and a finite element program (ANSYS® Multiphysics™, ANSYS, Inc., Canonsburg, PA (USA)). At a heating rate of 10 K/min the temperature difference between the centre of the sample and its surface was computed with 30 and 8 K, respectively. At temperatures above 900 °C the temperature difference between sample surface and furnace was less than 4 K (emissivity was 0.8). It was concluded that the temperature shift of the curves in figure 5 was not solely caused by different temperature gradients but also by kinetic hindrance of decomposition and shrinkage processes during faster heating.

The volume increase depended on heating rates. With 10 K/min it was about five times larger than with 2 K/min. The maximal density achieved before the onset of volume expansion was 30 % larger with a heating rate of 2 K/min than with 10 K/s (figure 6). From sintering science it is well known that closed pores are formed if the density reaches 88 to 94 % of theoretical density [21]. The release of gases within the sintering compacts leads to swelling effects since the gases can no longer escape to the surface via open pore channels [21]. If the formation of closed pores were the reason for the volume increase in the glass batches, it should start always at roughly the same density. The large change in the maximal density with heating rate (figure 6) showed that the phenomena which led to gas inclusions during heating of the glass batches were more complex.

In addition to the heating rate the composition of the batch also had a large influence on the volume change during heating. This can be seen from a comparison of type 1 and type 2 batches (figure 7). The total mass loss of both types corresponded to their respective carbonate concentrations. (The mass loss calculated from stoichiometry is indicated by the dashed lines in figure 7.) The additional glass fraction of type 2 batch speeded up shrinkage and weight loss. Type 2 batch showed an additional volume increase at about 900 °C (figure 7). Moreover, the local minimum in the volume curve was higher than with type 1 batch. Looking at sequential images of type 2 batch, formation and bursting of small bubbles (<1 mm) on the surface could be seen between 850 and 930 °C, which were absent in heating of type 1 batch. This implied that the additional volume

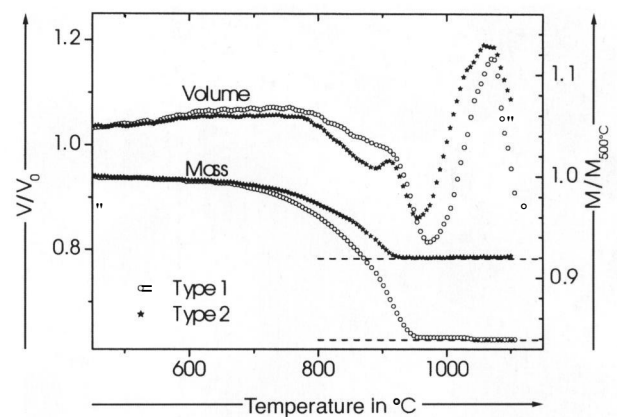


Figure 7. Volumetric and mass change during heating of type 1 and type 2 batch with 10 K/min.

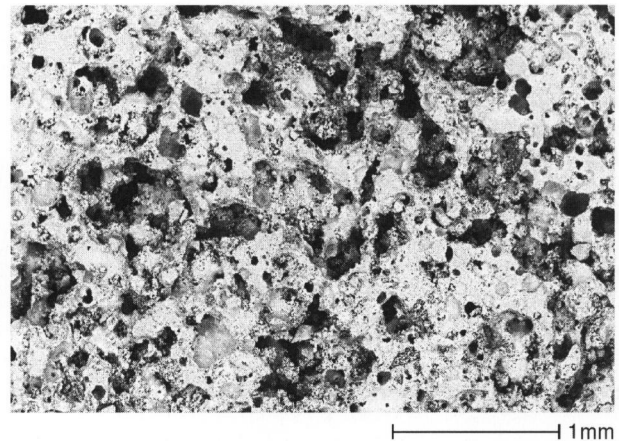


Figure 8. SEM micrograph of type 1 batch rapidly cooled down from a temperature of 900 °C to room temperature.

increase of type 2 batch at 900 °C was again caused by gas formation. It is likely that the additional glass fraction in type 2 batch became mobile and wetted residual solid carbonates. Therefore, further carbonate decomposition would have led to enclosed bubbles long before sintering had accomplished closed pores. This could explain the effect of heating rate on the density maximum which was observed in heating of type 1 batch as well (compare figure 5). Since wetting capability and mobility of melts increase with temperature, the kinetic shift of the decomposition reactions to higher temperatures with increasing heating rate would raise the fraction of carbonates which are covered by the melt and cannot release gases to the furnace atmosphere.

Figures 8 and 9 show SEM images from polished sections of type 1 and type 2 batch samples which were rapidly cooled down from a temperature of 900 °C. The pores appear dark and the solid particles can be identified by sharp edges. The liquid phase has a light grey appearance. It forms large clusters which enclose solid particles. The formation of those clusters is known from liquid phase sintering [22]. They are attributed to the decrease in interface energy when the interface area between liquid and gas is reduced by seg-

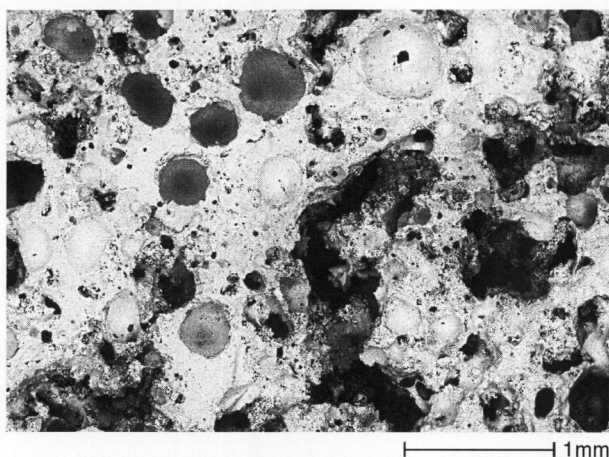


Figure 9. SEM micrograph of type 2 batch (50 % cullet) rapidly cooled down from a temperature of 900 °C to room temperature.

regation of the liquid phase in regions where it completely fills the pore channels. The clusters are larger in the sample containing cullet (figure 9) than in the sample without cullet (figure 8). Large bubbles are formed within the liquid phase. They can be identified by their spherical shape (figure 9). It is obvious that the gas could not be released to open pore channels from within the cluster. So the investigation of the microstructure confirmed the interpretation of volume increase which was given in the previous section.

5. Conclusions

A novel in situ measuring method has been developed which can detect volume and density changes during heating of glass batches. Although model samples had to be used in a small laboratory furnace, the sample volume was large enough to achieve a reasonable reproducibility. The method provides a sensitive tool for the characterization of glass batches with regard to their tendency to enclose gases during the melting process.

A comparison of different heating rates and batch compositions showed that density development depended on experimental conditions in a complex way. Our first results suggest that wetting and segregation by the liquid phase within the batch lead to an encapsulation of residual carbonates. Their decomposition form bubbles long before sintering has formed closed pores. Since the amount of remaining gas has a strong influence on the further processing of the glass melt and on the quality of glass production, more investigations on these phenomena are required.

The heating rates used in the present experiments were below the range of heating rates of industrial batch heating. Increasing the heating rate would lead to larger temperature gradients in the model samples. Obviously those gradients could no longer be neglected in the interpretation of the measuring data. Therefore, temperature gradients shall be included in our further investigations by in situ measurements of thermal diffusivity and thermal contact resistance of the batch heap. Moreover, this will allow for a better transfer of experimental results from the small model

samples in the laboratory furnace to the thick batch blanket in melting furnaces by finite element methods.

*

The authors gratefully acknowledge the help of R. Springer, W. Virsik, K. Olsowski, W. Hartmann with software development and furnace construction as well as the help of P. Michel, M. Römer and B. Schmid with the measurements.

6. References

- [1] Choudhary, M. K.; Huff, N. T: Mathematical modelling in the glass industry: an overview of status and needs. *Glastech. Ber. Glass Sci. Technol.* **70** (1997) no. 12, pp. 363–370.
- [2] Muschik, W.; Muysenberg, E.: Round robin for glass tank models. Report of the International Commission on Glass (ICG), Technical Committee 21 “Modelling of Glass Melts”. *Glastech. Ber. Glass Sci. Technol.* **71** (1998) no. 6, pp. 153–156.
- [3] Beerkens, R. G. C.: Modeling the kinetics of volatilization from glass melts. *J. Am. Ceram. Soc.* **84** (2001) no. 9, pp. 1952–1960.
- [4] Beerkens, R. G. C.: Advances in the modelling of the quality of glass melting processes. *Glastech. Ber. Glass Sci. Technol.* **74 C** (2001) pp. 83–129.
- [5] Fedorov, A. G.; Pilon, G.: Glass foams: formation, transport properties, and heat, mass, and radiation transfer. *J. Non-Cryst. Solids* **311** (2002) pp. 154–173.
- [6] Conradt, R.; Suwannathada, P.; Pimkhaokham, P.: Local temperature distribution and primary melt formation in a melting batch heap. *Glastech. Ber. Glass Sci. Technol.* **67** (1994) no. 5, pp. 103–113.
- [7] Buss, W.: Erhitzungsmikroskopische Untersuchungen von Vorgängen in Glasschmelzen mit und ohne Sulfat. *Glastech. Ber.* **35** (1962) no. 4, pp. 167–176.
- [8] Tammann, G.: *Der Glaszustand.*, Leipzig: Leonard Voss, 1933.
- [9] Boccaccini, A. R.: Sintering of glass matrix composites containing a particulate inclusion phase. *Adv. Compos. Letters* **4** (1995) pp. 143–149.
- [10] Winkler, S.; Davies, P.; Janoschek, J.: High-temperature dilatometer with pyrometer measuring system and rate-controlled sintering capability. *J. Therm. Anal.* **40** (1993) no. 3, pp. 999–1008.
- [11] Vidal, A.: Erforschung und kinematographische Untersuchung der Primärreaktionen der Gemengebestandteile im Hochtemperaturmikroskop. *Glastechn. Ber.* **36** (1963) no. 8, pp. 305–323.
- [12] Faber, A. J.; Beerkens, R. G. C.; de Waal, H.: Thermal behaviour of glass batch on batch heating. *Glastech. Ber.* **65** (1992) no. 7, pp. 177–185.
- [13] Wang, J.; Brewster, B. S.; McQuay, M. Q. et al.: Validation of an improved batch model in a coupled combustion space/melt tank/batch melting glass furnace simulation. *Glastech. Ber. Glass Sci. Technol.* **73** (2000) no. 10, pp. 299–308.
- [14] Raether, F.; Springer, R.; Beyer, S.: Optical dilatometry for the control of microstructure development during sintering. *Mat. Res. Innovat.* **4** (2001) pp. 245–250.
- [15] Sebastian, K.; Raether, F.; Springer, R.: TOMMI – A new instrument for the characterization of materials at high temperatures. *cfi/Ber. DKG* **80** (2003) pp. E91–E93.
- [16] Smrček, A.: European container glass 1982 to 1988. *Glastech. Ber.* **63** (1990) no. 10, pp. 309–317.
- [17] Kröger, C.: Gemengereaktionen und Glasschmelze. *Glastechn. Ber.* **25** (1952) no. 10, pp. 307–324.
- [18] Kröger, C.: Theoretischer Wärmebedarf der Glasschmelzprozesse. *Glastechn. Ber.* **26** (1953) no. 7, pp. 202–214.

- [19] Murai, S.; Wenzel, J.; Sanders, D. M.: Vaporisation in an unstirred soda-lime-silica glass melt. *Phys. Chem. Glasses* **21** (1980) pp.150–155.
- [20] Gebhardt, F.: Emissionen von Glasschmelzwannen und deren Minderung durch schmelztechnische Maßnahmen. *Glastechn. Ber.* **59** (1986) no. 12, pp. 344–349.
- [21] German, R. M.: *Sintering – theory and practice*. New York: John Wiley, 1996.
- [22] Kang, S.-J.K.; Kim, K.-H.; Lee, S.-M.: Theoretical analysis of final stage liquid-phase sintering; *Sintering Technology* (1995). New York: Dekker, 1996. Pp. 221–228.

■ E304P003

Contact:

Dr. Friedrich Raether
Fraunhofer ISC
Neunerplatz 2
D-97082 Würzburg
E-mail: raether@isc.fhg.de